BBA - Bioenergetics 1860 (2019) 1–11

Contents lists available at ScienceDirect

BBA - Bioenergetics

journal homepage: www.elsevier.com/locate/bbabio

Elimination of proton donor strongly affects directionality and efficiency of proton transport in ESR, a light-driven proton pump from *Exiguobacterium sibiricum*

Sergey A. Siletsky[a,*], Mahir D. Mamedov[a], Evgeniy P. Lukashev[b], Sergei P. Balashov[c,**], Dmitriy A. Dolgikh[b,d], Andrei B. Rubin[b], Mikhail P. Kirpichnikov[b,d], Lada E. Petrovskaya[d,***]

[a] Belozersky Institute of Physical-Chemical Biology, Lomonosov Moscow State University, 119991 Moscow, Russian Federation
[b] Department of Biology, Lomonosov Moscow State University, 119234 Moscow, Leninskie gory, 1, Russian Federation
[c] Department of Physiology and Biophysics, University of California, Irvine 92697, USA
[d] Shemyakin & Ovchinnikov Institute of Bioorganic Chemistry, Russian Academy of Sciences, 117997 Moscow, Ul. Miklukho-Maklaya, 16/10, Russian Federation

ARTICLE INFO

Keywords:
Retinal protein
Light energy transduction
Proton pump
Photocycle
Photoelectric potential generation
Charge transfer steps
Back reactions

ABSTRACT

ESR from *Exiguobacterium sibiricum* is a retinal protein which functions as a proton pump. Unusual feature of ESR is that a lysine residue is present at a site for the internal proton donor, which in other proton pumps is a carboxylic residue. Replacement of Lys96 with alanine slows reprotonation of the Schiff base by two orders of magnitude, indicating that Lys96 and interacting water molecules function as internal proton donor to the Schiff base. In this work we examined time resolved generation of light-induced electric potential ΔΨ by the K96A mutant reconstituted into proteoliposomes. We found that the ΔΨ component, which accompanied reprotonation of the Schiff base in wild type ESR, was not only slowed but also decreased greatly in the mutant, and negative phase appeared at high pH. This indicates a higher probability of back reactions in ESR than in bacteriorhodopsin since no negative components have been observed in homologous mutants of BR, D96N and D96A. The higher rate of back reactions in ESR is probably caused by different arrangement of the proton acceptor site compared to that in BR and different sequence of proton release and uptake. Addition of sodium azide, which substitutes for the internal proton donor, restores both the rate and amplitude of the ΔΨ components related to the Schiff base reprotonation in the K96A mutant. This indicates that overall proton transport results from competition of forward and reverse reactions, and emphasizes the importance of internal donor for high efficiency and directionality of H^+ transfer.

1. Introduction

Development of genomic and metagenomic research revealed that retinal containing microbial proton pumps are wide spread and contribute considerably for capturing and utilization of light energy [1–3]. This is largely due to the role of these pumps as light energy transducers helpful for survival of microorganisms, and relative simplicity of these pumps, where proton transport occurs in a single protein. It is driven by the retinal chromophore photoisomerization, which initiates a cycle of protein changes coupled to proton translocation through the interior of a protein. Intensive studies of bacteriorhodopsin of Archaea [4–12] led to understanding of the main features of proton transport mechanism, which involves transient deprotonation of the retinal protein Schiff base in the M intermediate [13] and protonation changes of internal proton acceptor and proton donor, which both are aspartic acid residues [14–16], and of proton release complex [17–19].

Discovery of novel natural variants of proton pumps, proteorhodopsins of marine proteobacteria [1] and xanthorhodopsins from

Abbreviations: BR, bacteriorhodopsin; ESR, retinal protein from *Exiguobacterium sibiricum*; PR, proteorhodopsin; XR, xanthorhodopsin; DDM, *n*-dodecyl-β-D-maltopyranoside; OG, *N-Octyl*-β-D-*glucoside*; HEPES, 4-(2-hydroxyethyl)piperazine-1-ethanesulfonic acid; MES, 2-(*N*-morpholino)ethanesulfonic acid; PRG, proton release group (complex)

* Corresponding author.
** Correspondence to: S.P. Balashov, Dept. of Physiology and Biophysics, C-335 Medical Sciences I, University of California, Irvine, CA 92697-4560, USA.
*** Correspondence to: L.E. Petrovskaya, Shemyakin and Ovchinnikov Institute of Bioorganic Chemistry, ul. Miklukho-Maklaya, 16/10, 117997 Moscow, GSP-7, Russian Federation.
E-mail addresses: siletsky@genebee.msu.su (S.A. Siletsky), balashov@uci.edu (S.P. Balashov), lpetr65@yahoo.com (L.E. Petrovskaya).

https://doi.org/10.1016/j.bbabio.2018.09.365
Received 30 June 2018; Received in revised form 31 August 2018; Accepted 16 September 2018
Available online 18 September 2018
0005-2728/

Bacteroides group [20] revealed several structural modifications in the proton transfer pathways of these proteins. A new component, His, closely interacting with the aspartate proton acceptor, appeared at the extracellular side of these eubacterial pumps, whereas a specialized proton release complex was absent [21,22]. In the cytoplasmic side, the internal proton donor (Asp96 in bacteriorhodopsin) was replaced with Glu.

Unusual substitution was found in a gene of a protein called ESR [23] from *Exiguobacterium sibiricum*, an organism found in Siberian tundra permafrost [24], and in the genes of the related *Exiguobacterium* species [25]. Lysine (Lys96) was present in the donor site, which usually contains carboxylic residues, either Asp or Glu in pumps from archaea and eubacteria, respectively. Studies of the ESR protein, expressed in *Escherichia coli*, have shown that it is a proton pump [23,26]. Crystal structure of ESR indicates that Lys resides in a cavity surrounded by hydrophobic residues and interacts with a water molecule [27]. Substitution of Lys96 with nonionizable residues decreases the rate of the Schiff base reprotonation by 100–500 times [28] indicating that Lys96 facilitates the delivery of a proton from the cytoplasmic side to the Schiff base in ESR during the M to N transition. The kinetic studies suggest that Lys96 is neutral in the initial state. Upon deprotonation of the Schiff base in the M intermediate, proton uptake from the cytoplasmic side takes place, Lys96 and/or associated water molecule undergoes transient protonation followed by proton transfer to the Schiff base. This results in a different sequence of events compared to other proton pumps with carboxylic residues in a donor site, in which proton transfer from a donor to the Schiff base precedes proton uptake from the bulk. A different way of operation of Lys in the donor site causes also an altered pH dependence of the M and N intermediates kinetics [28] and associated electrogenic phases [29]. Elimination of the donor site by substitution of Lys96 with Ala in the K96A mutant caused more than two orders of magnitude slowing of the Schiff base reprotonation [28,30] and a substantial decrease in the rate of proton pumping in *E. coli* cells, especially at high pH [28].

In this paper we examined photoelectric responses from the K96A mutant reconstituted in proteoliposomes and showed that this mutation caused not only slowing of the Schiff base reprotonation but also a decrease in the yield of proton transport apparently from back reactions. It appears that they effectively compete with proton transfer from cytoplasm to the Schiff base when the donor is missing. This is different from the effect of analogous mutation of bacteriorhodopsin, D96A, which also slows the Schiff base reprotonation but does not cause decrease in its yield substantially. The likely origin of these differences and back reactions affecting overall directionality of transport are discussed.

2. Materials and methods

2.1. Expression of ESR and K96A mutant and their reconstitution into phospholipid liposomes

ESR was expressed in *E. coli* BL21(DE3)pLysS and purified according to [23]. The K96A mutant was constructed and expressed as in [26]. For preparation of proteoliposomes the protein was solubilized in OG from Anatrace (USA). Other chemicals were from Sigma and Panreac (Spain). Liposomes were produced from azolectin (20 mg/ml Sigma, type IV-S, 40% w/w phosphatidylcholine content) by sonication at 22 kHz, 60 μA for 2 min in 1 ml of 25 mM HEPES-NaOH buffer, pH 7.5. Reconstitution of ESR and its K96A mutant into proteoliposomes was carried out as previously [29] by mixing the liposomes with ESR in 1.5% (w/v) OG at the lipid/protein ratio of 100:1 (w/w) for 30 min in the dark. The detergent was removed by addition of 20-fold excess (by weight) of Bio-Beads SM-2 (Bio-Rad) and stirring the suspension for 3 h at room temperature. The proteoliposomes were separated from Bio-Beads® by decanting. The proteoliposomes were pelleted at 140,000 g at 4 °C for 1 h in a Beckman L-90K ultracentrifuge and resuspended in 25 mM MES-NaOH (pH 6.5) buffer. Reconstitution of ESR into liposomes was with high degree of unidirectional orientation, as follows from large light-induced potential changes observed in this and previous study [29].

2.2. Spectroscopic characterization

Flash-induced time resolved absorption changes of ESR and its mutant in suspension of proteoliposomes were examined with lab-made flash-photolysis system as in [29]. Prior to measurements, all samples were adjusted to $A_{530} = 0.1$. Flashes (532 nm, 8 ns, 10 mJ) were from LS-2131M Nd-YAG Q-switched laser (LOTIS TII, Belarus). Transient absorption changes were detected by photomultiplier and digitized by Octopus CompuScope 8327 (GaGe, Canada). Kinetic traces were fit with a sum of exponentials using Mathematica (Wolfram Research, USA).

2.3. Electrometric time-resolved measurements of the membrane potential generation

Generation of the transmembrane electric potential difference ΔΨ was studied using an electrometric setup [31] with time resolution of 100 ns as described in [29,32]. This technique includes fusion of proteoliposomes with the surface of a collodion phospholipid-impregnated film (a membrane), which separates two sections of the measuring cell filled with a buffer solution. A pulsed Nd-YAG laser (YG-481, Quantel, λ = 532 nm) was used as a source of flashes. In the process of light-driven proton transfer, ESR creates ΔΨ across the vesicle and the measuring membranes, which is detected by Ag^+/AgCl electrodes immersed in a solution at different sides of the latter membrane. The membranes have low conductivity (high resistance of 2–3 GOhm) [6] so the light-induced ΔΨ decays passively in the dark with a time constant of about 1 s at neutral and high pH.

2.4. Electrometric data analysis

The kinetic traces were resolved into individual exponents using program packages Pluk [33], Origin (OriginLab Corporation, USA) and MATLAB (The Mathworks, South Natick, MA), as it has been done initially for the photoelectric responses of the wild type and mutant forms of bacteriorhodopsin, cytochrome oxidase and others proteins [6,32,34–40]. This provides true time constants of the phases, whereas the interpretation of the relative amplitudes depends on the kinetic model employed [41,42]. The intrinsic amplitudes of the electrogenic steps are simply equal to those found by deconvolution of the electrometric curves, if the electrogenic phases are related to parallel processes or differ in rates significantly. If the phases are associated with consecutive processes, the relative amplitudes of the phases can be substantially affected when the rates of the processes differ by less than one order of magnitude [41–43]. The relative amplitudes of the electrogenic phases for the serial model can be estimated by recalculation according to work [41,42].

3. Results

The kinetics of light-induced changes of transmembrane potential difference (ΔΨ) for ESR containing proteoliposomes attached to a collodion film were examined for the wild type and K96A mutant at pH values between pH 6.5 and 8.5 along with the light-induced absorption changes of proteoliposomes at selected wavelengths, as described below.

3.1. Effect of K96A mutation on the photoelectric response ΔΨ at pH 7.5

Fig. 1 shows the kinetics of generation of membrane potential (ΔΨ) in wild type ESR and the K96A mutant at pH 7.5. Light-induced absorption changes in proteoliposome suspension with wild type and the

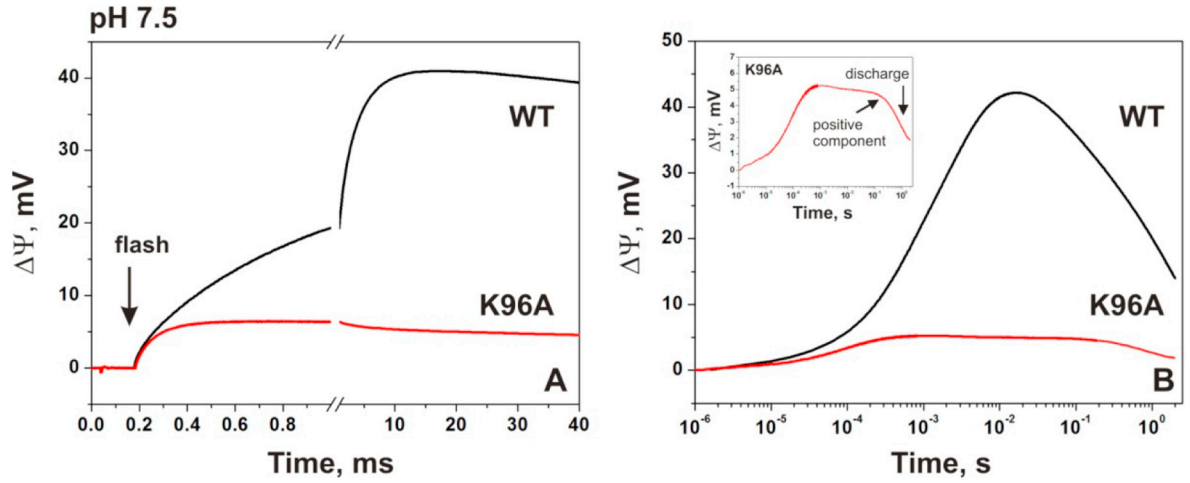

Fig. 1. Kinetics of light-induced changes in membrane potential difference, ΔΨ, in proteoliposomes containing wild type ESR and K96A mutant. A) Photoelectric curves are shown in a linear time scale during the first 40 ms, when large buildup of ΔΨ takes place in the wild type. B) Plot on logarithmic time scale up to 2 s after the flash, which includes the decay of the ΔΨ due to passive leak of the membrane. Inset: The photoelectric response of K96A mutant. The small positive electrogenic phase and passive discharge are shown with arrows.

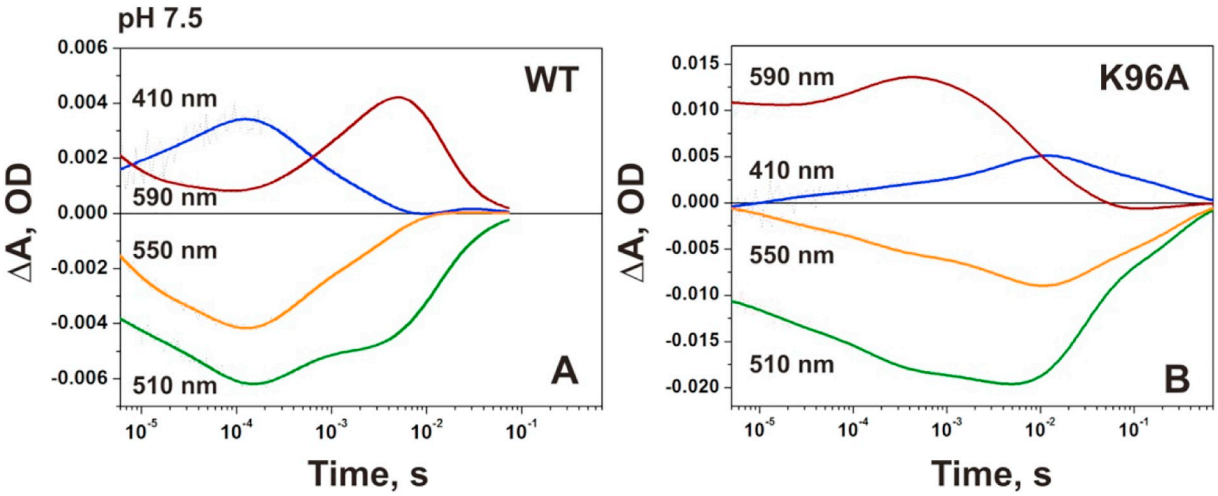

Fig. 2. Light-induced absorption changes at four characteristic wavelengths (410 nm, 590 nm, 550 nm and 510 nm) at pH 7.5 in proteoliposome suspensions containing: A) Wild type ESR. B) K96A mutant.

K96A mutant are depicted in Fig. 2. The results of the fit of the kinetic traces are presented in Tables S1 and S2.

As one can see from Fig. 1, the K96A mutation eliminates major positive electrogenic phases, which correspond to the Schiff base reprotonation (M decay) and initial state (ESR) recovery as comparison with spectral data indicates (see below). This is an unexpected result since slowing of millisecond phases related to the Schiff base reprotonation by two orders of magnitude is expected but not their disappearance. Below we describe the changes caused by the K96A mutation in comparison with the wild type ESR at pH 7.5 in more details.

A photoelectric response from the wild type ESR-containing proteoliposomes exhibits phases in microsecond and millisecond time range. The sign of the ΔΨ generation corresponds to the transfer of a positive charge from the interior of the proteoliposomes to the bulk phase. In the wild type, the flash-induced photopotential increases up to ~30 ms, then it slowly decreases from a passive discharge of the membrane and returns to the initial level on the time scale of several seconds. The kinetics of ΔΨ in the mutant is similar to that of the wild type only at early part of the photocycle, during first ca. 100 μs after the flash. The larger and slower (millisecond) positive phases of the photoelectric response are missing. The maximum amplitude of the response obtained in the experiments with K96A mutant was ~6 mV. Typical values of the total amplitude of ΔΨ were ~7–10 times less than in wild type.

Six positive components are resolved in the kinetics of ΔΨ generation in the wild-type (Table S1). They include the major electrogenic processes coupled to the formation of the M state and the M → N1, N1 → N2 (O) and N2 (O) → ESR transitions [29]. Three components (3 μs, 24 μs, and 100 μs) are coupled with the formation of M (see below). Their total amplitude is about 6%. This is somewhat less than expected from the transfer of a proton from the Schiff base to the primary acceptor (9%). This is because a slower component of M rise might be present (described below and in Table S2) and because there is a contribution from negative components with a close time constant in the initial part of the photocycle [29]. These negative phases, present also in the photoresponse of bacteriorhodopsin, are associated with the early intermediates (K and L) of the cycle [6].

In the absorption kinetics (Fig. 2A), the formation of M is accompanied by an increase in absorption at 410 nm with rate constants 3 μs, 14 μs, and 82 μs, similar to those seen in kinetics of ΔΨ, which reflect Schiff base deprotonation and transfer of a proton to Asp85. This is preceded by formation of the K and L intermediates. The formation of the K intermediate in the initial part of the ESR photocycle is reflected by the unresolved changes of absorbance upon the flash at the 590 nm

and 510 nm, whereas decay of the K intermediate and formation of the L intermediate occurring on the microsecond time scale are accompanied by the decrease of absorption at 590 nm, 550 nm and 510 nm.

The subsequent two components of ΔΨ occur in a millisecond time scale (0.6 ms and 3.4 ms) and make the main contribution to electrogenesis. They reflect the transfer of protons through the input proton channel from the bulk to the Schiff base during the decay of the M intermediate which occurs in two transitions M ↔ N1 → N2/O, with time constants 0.57 and 2.6 ms. It manifests as the decrease of absorption at 410 nm and concurrent increase at 510 nm, 550 nm and 590 nm [28]. The decay of the N2/O state into the initial ESR is accompanied by a decrease of absorption at 590 nm and concurrent increase at 510 nm with time constant 21 ms (Fig. 2A). This step corresponds to the slowest positive electrogenic phase (~18.4 ms), which reflects reisomerization of the chromophore, deprotonation of proton acceptor Asp85 and release of a proton to the outer side of the membrane. The transitions M → N1 → N2/O and N2/O → ESR produce major contribution to the amplitude of the light-induced membrane potential ΔΨ, ca. 90%.

These major millisecond electrogenic phases are missing in the K96A mutant (Fig. 1) and decay of electric potential starts earlier than in the WT (Fig. 1B, inset). The accumulation of the red shifted N/O intermediates, which in WT appear along with the M decay, is also missing, as seen in Fig. 2A, the 590 nm trace. This is caused by slowing of the decay of the M intermediate by more than 100 fold. Best fit of M decay in K96A includes two kinetic components, 28 ms and 283 ms (Table S2). The dramatic slowing of the M decay and Schiff base reprotonation has been demonstrated for the K96A earlier [28,30], but elimination of the millisecond electrogenic phases is a new surprising finding. It is not caused by slowing of the M decay. If the photocycle is slowed down but proceeds through the same pathway as in the WT, the major electrogenic phases should be detectable, as shown in a simulation presented in Fig. 3. To understand the reason for the lack of major electrogenic phases in the K96A mutant, we analyzed its kinetics in more detail and examined their pH dependence. We found (see below), that this phenomenon persists at all pH values between 6.5 and 8.5 (Fig. 4B).

In the microsecond time range, three positive components with time constants 3 μs, 70 μs and 220 μs comprise the photoelectric response in the mutant associated with transfer of a proton from the Schiff base to Asp85 during formation of the M intermediate. They are similar to analogous components in the wild type (see Table S2) except the time constants of the latter two are two times slower. In the kinetics of M rise (Fig. 2B), besides these fast components, a slower, 5 ms component is present, which is not seen in the wild type, probably because of a faster decay of M. It was not accompanied by a corresponding increase in ΔΨ, rather a negative electrogenic phase was observed with a similar time constant (Table S2).

The fit of photoelectric response in the mutant in the millisecond time domain reveals three small phases, 2.2 ms, 25 ms and 137 ms. The first two are negative. The 2.2 ms phase likely corresponds to 5 ms component of M rise and the second, 23 ms, corresponds to the fast component of M decay in the mutant. The negative sign of the 23 ms component indicates that reprotonation of the Schiff base occurs not from the cytoplasmic surface but rather from the extracellular side. The positive 137 ms component correlates with the slower component of M decay with time constant 283 ms (Table S2, Inset to Fig. 1B and Fig. 4). Remarkably, the amplitude of the 137 ms phase is very small; it is less than 2% of the amplitude of ms phases in the WT. This suggests that it is either caused by a small charge movement (perhaps transfer of a proton to the Schiff base from some nearby water molecule) or probably it is a sum of positive and negative phases which largely cancel each other. Appearance of these negative and small positive phases is peculiar to the mutant. In the wild type, the last positive component of 18.4 ms is followed by almost monophasic decay from a passive discharge of the membrane with a time constant of ca. 1 s. A complex decay of ΔΨ in K96A is shown in Fig. 1B. The different sign of millisecond components associated with M decay indicates that reprotonation of the Schiff base in K96A occurs from different sources. The 137 ms positive component is likely to include at least partially the “normal” source, the proton diffusion from the cytoplasmic side. The negative phases suggest movement of H^+ in the opposite direction.

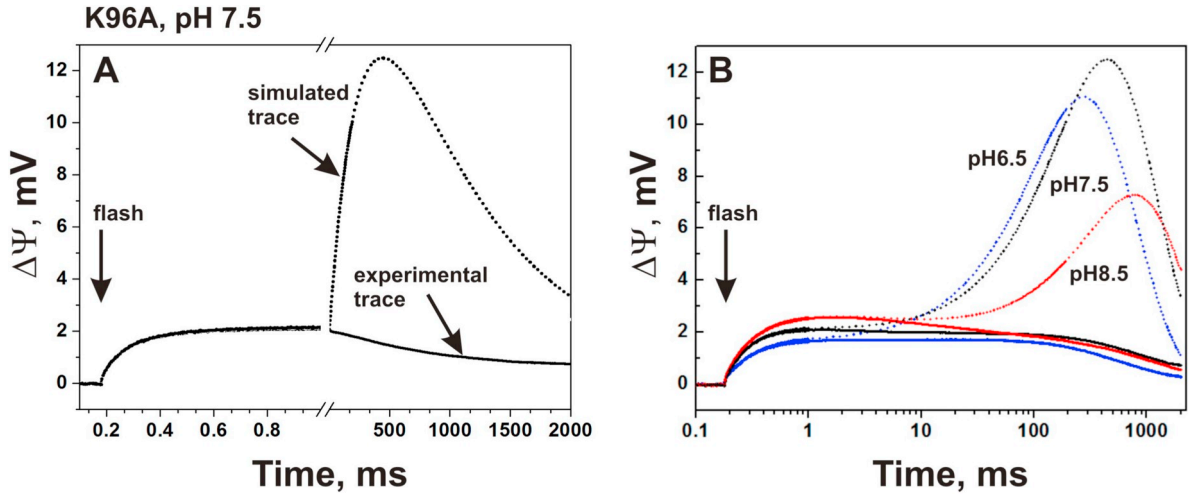

Fig. 3. The measured (solid lines) and simulated (dotted lines) kinetics of membrane potential generation by the K96A mutant. A) pH 7.5, linear scale. B) pH 6.5, 7.5 and 8.5, logarithmic scale. In the simulation it was assumed that reprotonation of the Schiff base occurs in the same way and through the same intermediates as in WT but about 100 times slower. The presence of large millisecond positive phase in simulated curves indicates that slowing of the Schiff base reprotonation by itself would not cause its disappearance and should be detectable. The lack of this phase indicates that reprotonation of the Schiff base in M of K96A occurs without generation of significant positive phase of ΔΨ and apparently involves reverse proton transfers. The simulated curves for the K96A mutant were obtained by adding to the experimentally observed curves the calculated kinetics of components of ΔΨ coupled to the M decay based on the fact that the total amplitude of all the components of ΔΨ associated with the decay of M to the initial state is 9 times greater in wild type ESR than the electrogenic processes accompanying the formation of M. For each of the pH values, the slowest of the two time constants for the M decay was used. This resulted in the lowest amplitude of the simulated photoelectric response. The contribution from the discharge of the membrane (using the experimentally monitored characteristic time constants of passive membrane leakage) was taken into account assuming that the generation of ΔΨ and its decay are consecutive events. The formula for ΔΨ(t) associated with M decay can be described as $\Delta\Psi(t) = \Delta\Psi o\ k_1/(k_1\text{-}k_2)\ (e^{-k1t}\text{-}e^{-k2t})$ [42]. The two models produced similar kinetics (curves 1 and 2, respectively) both showing a large component of ΔΨ(t) corresponding to M decay. For the Fig. 3B simulation was done using the second formula. The results indicate that in the absence of shunts and back reactions the potential generation corresponding to M decay should be detectable at all three pH values, even if it is slowed 100 fold.

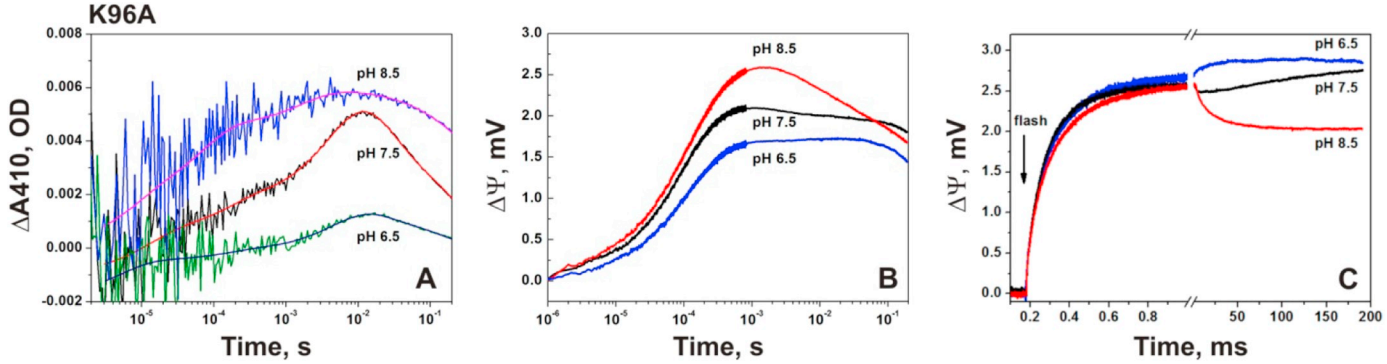

Fig. 4. Effect of pH on: A) Kinetics of absorption changes at 410 nm from formation and decay of the M intermediate in the suspension of proteoliposomes with the K96A mutant. B and C) Kinetics of membrane potential generation by K96A; C) Same as B but passive discharge of the membrane (~900–1000 ms component) was subtracted from the experimental traces. The traces were normalized at the 1 ms point and plotted on a linear time scale.

3.2. pH dependence of electrogenic phases in K96A

Investigation of the pH dependence of electric components of the K96A mutant could be helpful in understanding the nature of almost complete elimination of the phase corresponding to the M decay. Earlier studies showed that the rate constant of the Schiff base reprotonation (M decay) in the K96A mutant linearly depends on bulk proton concentration with a slope of 0.63 in the lipid like detergent LPG [28] and with somewhat lower slope of 0.5 in proteoliposomes [30]. The deviation from the theoretical slope 1 was also observed for analogous bacteriorhodopsin mutants and was tentatively associated with influence of surface charges [44].

The rate of deprotonation of the Schiff base (M formation) is also pH dependent both in the wild type and K96A mutant. The rates of M formation and accumulation increase in a titration-like manner with a pK_a, which depends on environment. It is ca. 9 in DDM [26], 6.3 in LPG [28] and 7 in proteoliposomes [30]. This transition correlates with 9 nm blue shift of the absorption maximum in the initial state at high pH. Both transitions were tentatively attributed to the pK_a of His57, which makes a strong hydrogen bond with Asp85 in the initial state [26] and is in position to affect its proton affinity.

The measurements of light-induced pH changes in suspension of *E. coli* cells showed decreased rates of proton transfer of K96A [28]. They were only 30% or less of that in WT at pH between 6 and 7 and less than 10% at pH 8.2, which could be caused by a slower photocycle, or less efficient photocycle or both. Study of the pH dependence of electrogenic phases together with photocycle transitions under single flash excitation can potentially clarify that.

Fig. 4A shows that in agreement with previous observations in liposomes [30], large changes in the kinetics of M formation and decay are observed upon increase in pH. At pH 6.5 the major component of the M rise is slow (rise time is 5.6 ms), which correlates with long lifetime of the K-like intermediate (trace 590 nm in Fig. 5B). In contrast to that, at pH 8.5 the fast component of M rise dominates with τ 6.8 μs and 67 μs, and the K intermediate decays completely by 10 ms after the flash (trace 590 nm in Fig. 5D). The M decay is accelerated ca. 1.7 fold at pH 6.5 and slowed about 4.6 fold at pH 8.5 compared to that at pH 7.5 (Table S2).

Fig. 4B and C depict the kinetics of the light-induced electric potential at three pH values in the K96A mutant on logarithmic and linear scales. Several features are important. The pH dependence of early phases of M rise (Fig. 4A) is reflected in the photoelectrical changes ΔΨ (see Table S2), however the overall amplitude of the positive components of ΔΨ is less pH dependent than the amplitude of M. A likely explanation for this is the involvement, besides the H^+ transfer from the Schiff base to Asp85, of other electrogenic processes at lower pH, particularly deprotonation of His57, as suggested earlier [26]. The second important feature is that a small positive component of ΔΨ in millisecond range is present at pH 6.5 and at pH 7.5 but is not detectable at pH 8.5. Rather the negative components with τ ~6.9 ms and 29 ms are present. This is especially obvious after subtraction of the kinetics of passive discharge as shown in Fig. 4C. Only a decrease in potential is observed in the millisecond timescale for the pH 8.5, whereas at pH 7.5, in addition to fast millisecond negative phases, a small positive electrogenic process (~137 ms) is observed (Fig. 4B and C, Table S2). At pH 6.5, only a positive electrogenic component is resolved with τ ~17 ms (Table S2) in this time interval. However, the amplitude of this positive electrogenic component does not exceed a few percent of the total response in the wild type, similar to that at pH 7.5. These data suggest that two different pathways are involved in reprotonation of the Schiff base in the K96A mutant, one through the cytoplasmic channel, which is more efficient at low pH, and the other is from the extracellular side, which is predominant at high pH. If they are in competition, then accelerated delivery of a proton through the cytoplasmic channel should lead to larger positive electric components. This indeed happens in the presence of sodium azide (see below).

The spectral changes of the mutant at pH 6.5, measured at four wavelengths, resemble those at pH 7.5 (Fig. 5B). Their difference from the wild type (Fig. 5A) is mainly due to the slowdown of the M formation and decay due to the mutation. However, it is worth noting the following details. The main phase of the increase in absorption at 410 nm (~5 ms) occurs in parallel with the decrease in absorption at 510 and 590 nm. These changes are characteristic of the formation of M, which occurs slowly at low pH and is limited apparently by the deprotonation of His57 or other interacting residue. The decay of M is characterized by a decrease in absorption at 410 nm and a simultaneous increase in absorption at 510 nm, which occur with two characteristic times (16 ms and 150 ms). Only the first of these components is accompanied by a positive phase of ΔΨ with τ ~15 ms and small amplitude of ~6%, which reflects electrogenic process coupled to the M → N2/O → ESR transformations. It is the case only for the rapid component of M decay. Apparently, reprotonation of the Schiff base during the 159 ms phase of M decay occurs in such a way that contributions of the positive component from direct proton transfer from cytoplasmic surface and negative components from a reverse proton transfer from the primary acceptor cancel each other and do not produce a significant elecrogenic current.

At pH 8.5, the residue (presumably His57) affecting proton affinity of the proton acceptor Asp85, is deprotonated already in the initial state. This results in fast and almost complete decay of the K and L intermediates into M mostly in microsecond time range (Fig. 5D). This simplifies the photocycle. Comparison of kinetics of absorption changes at 410 nm with that of ΔΨ in the mutant at pH 8.5 shows that ΔΨ increases simultaneously with the rise of M, unlike at pH 6.5 where M accumulation occurred with some delay. The decay rate of M slowed to 1.15 s vs 2.7 ms in WT and more than 5 fold compared to pH 7.5. The

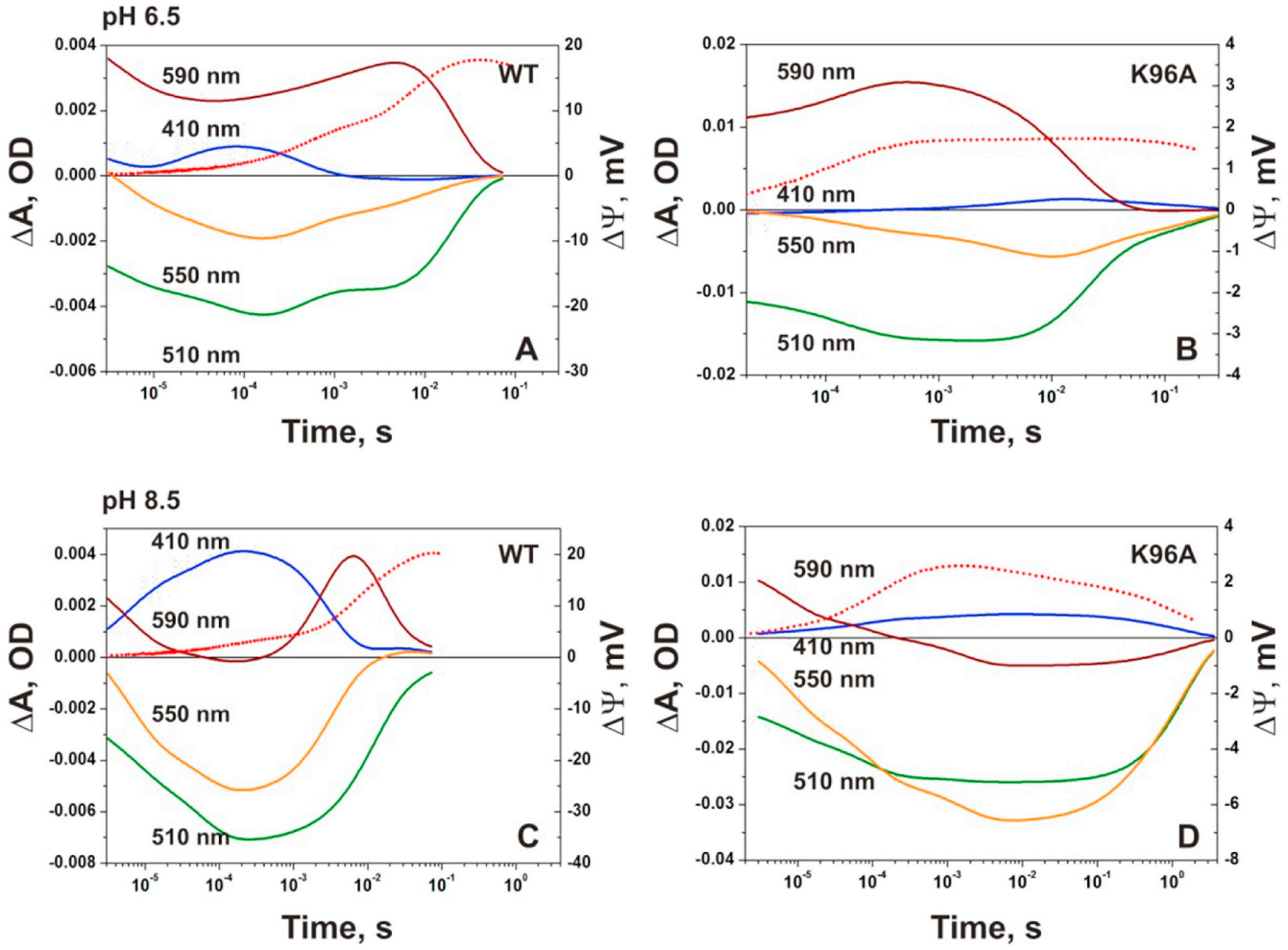

Fig. 5. Light-induced absorption changes of wild type and K96A mutant at four characteristic wavelengths (410 nm, 590 nm, 550 nm and 510 nm) at pH 6.5 (A, B) and 8.5 (C, D). Dotted lines are the corresponding photoelectric responses (ΔΨ).

latter suggests that the limiting process in M decay is the transfer of a proton from the bulk. However, unlike in the wild type, the decay of M is not accompanied by a significant positive electrogenesis. It is possible that some very small positive component is still present but masked by two negative ones, which occur with τ 6.9 ms and 29 ms and passive membrane discharge (~1000 ms).

3.3. Effect of sodium azide on the kinetics of membrane potential generation in the K96A mutant

Azide accelerates Schiff base reprotonation and M decay in the K96A mutant of ESR [28] as it does in bacteriorhodopsin [45–47]. Here, we examined the effect of azide on ΔΨ generation in the photocycle of the K96A mutant of ESR. Addition of 1 mM of sodium azide does not affect the microsecond part of the kinetics but in a millisecond time range, a small positive component of ΔΨ appears (Fig. 6A). Addition of 80 mM NaN_3 results in appearance of large positive electrogenic phases in millisecond time range with characteristic time constants of 6 ms and 21 ms. The kinetics of ΔΨ in the mutant in the presence of high concentration of NaN_3 resembles that of the WT (Fig. 1A), indicating that azide substitutes for the missing Lys96, and to a large extent restores the component of ΔΨ corresponding to the M decay in the mutant along with fast delivery of protons from the bulk to the Schiff base, as indicated by acceleration of M decay (Fig. 6B). In the WT, the constants corresponding to the 6.2 ms component of ΔΨ in 80 mM sodium azide are 0.6 ms and 3.4 ms (Tables S1 and S2).

As one can see in Fig. 6B, addition of NaN_3 resulted in faster decrease in absorption at 410 nm and increase at 550 nm and at 590 nm as compared to that in the mutant without azide (Fig. 2B). These absorption changes correspond to the transitions M → N1 → N2/O, developing with a characteristic time 5.6 ms, close to that of the 6.2 ms electrogenic phase. They involve reprotonation of the Schiff base from the cytoplasmic side. The rate of the second millisecond electrogenic phase (~21 ms) is close to the rate of the decrease of absorption at 590 nm and parallel increase at 510 nm. These changes of absorbance and the parallel electrogenic step reflect the N2/O → ESR transition, in which Asp85 deprotonates and a proton is released to the extracellular surface. In the presence of 80 mM azide the Schiff base protonation is not a rate limiting step in the sequence of transformations M ↔ N1 → N2/O → ESR, being faster than the last step. This allows some accumulation of the N2/O state, which is seen as a small absorption increase at 590 at 10 ms, but not as prominent as in the WT (Fig. 2A).

Thus, the effect of azide on the kinetics of generation of membrane potential by the K96A mutant of ESR is similar to its effect on the D96N mutant of bacteriorhodopsin [46,48], in both cases causing the acceleration of the M decay coupled to the Schiff base reprotonation. A significant difference, however, is that in the case of the K96A mutant, azide not only accelerates reprotonation of the Schiff base, but also restores the amplitude of the millisecond electric phases and thus the efficiency of proton transport. A likely reason for that are differences in the structure of proton transfer pathways and mechanisms of BR and ESR as discussed below.

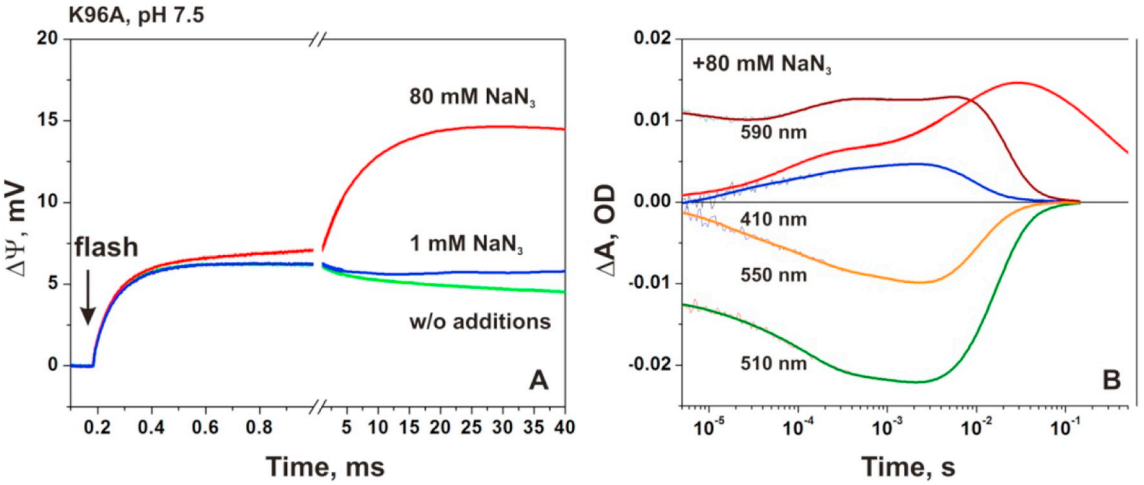

Fig. 6. Effect of sodium azide on the kinetics of light-induced membrane potential generation and M decay in the K96A mutant at pH 7.5. A) ΔΨ generation in no azide; 1 mM sodium azide; and 80 mM sodium azide. B) Light-induced absorption changes of K96A and kinetics of ΔΨ (red line) in the presence of 80 mM NaN_3.

4. Discussion

The unexpected and surprising finding of this study is that substitution of Lys96, which is at the internal donor site in ESR, with alanine, not only greatly slows reprotonation of the Schiff base, but affects directionality and quantum efficiency of the proton transfer. In the K96A mutant, positive phases of electric potential generation, which are normally coupled with the reprotonation of the Schiff base during the decay of the M intermediate are greatly decreased and negative components appear, especially noticeable at pH 8.5 (Fig. 4, Table S2). This suggests that reprotonation of the Schiff base in the mutant occurs mostly from the extracellular side rather than from the cytoplasmic side, probably in a reverse proton transfer from Asp85 back to the Schiff base and due to proton transfers from the bulk phase to the Asp85-His57 site as shown in Fig. 7. Even at pH 6.5, the amplitude of positive component related to the M decay in the mutant is small. This finding explains the earlier observation that proton pumping rate of the K96A mutant in *E. coli* cells is decreased compared to that of WT ESR more than 2.5 fold at neutral pH and more than 10 fold at pH 8 [28].

4.1. Origin of reverse reactions which reduce efficiency of proton transport in the K96A mutant of ESR

The normal amplitude of the positive components coupled to the M decay was restored in the mutant by addition of sodium azide (Fig. 6), which speeds up decay of the M intermediate, facilitating delivery of protons to the Schiff base from the cytoplasmic surface. This suggests that the efficiency of proton transport depends on a competition of a transfer from cytoplasmic surface to the Schiff base with opposite transfers from the extracellular side, and is apparently proportional to a ratio of the rates of the forward, k_f, and reverse (or shunt), k_r, reactions, $k_f/(k_f + k_r)$. The reverse reaction(s) become important when the rate of proton delivery to the Schiff base from the cytoplasmic side slows greatly and become comparable to the rates of the reverse reactions. The total electric potential generated during the decay of M would be a sum of the two processes, forward and reverse and the positive phase of ΔΨ, related to the Schiff base reprotonation would be greatly reduced when $k_f < k_r$ and even reversed, as observed at pH 8.5. The reactions, which might be involved in these reverse and shunt pathways were observed in bacteriorhodopsin and shown by analogy in the scheme below.

$$\mathrm{K96A} \Rightarrow \mathrm{K} \rightarrow \mathrm{L} \leftrightarrow \mathrm{M} \leftrightarrow \mathrm{N1} \rightarrow \mathrm{N2/O} \rightarrow \mathrm{K96A}$$
$$\downarrow$$
$$\mathrm{K96A}$$

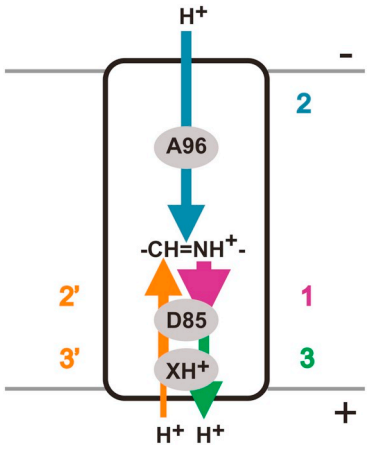

Fig. 7. Proton transfers coupled to major electrogenic steps during the photocycle of the K96A mutant of ESR. 1 (purple arrow), from the Schiff base to the primary acceptor Asp85; 2 (blue arrow), from the cytoplasmic surface to Schiff base; 3 (green arrow), from Asp85 to the extracellular side through the X (His57 or other interacting residue); 2′ and 3′ (orange arrow) reverse reactions involving transfer of a proton from the extracellular side through X and Asp85 to the Schiff base. The overall transport is a result of competition of forward and reverse reactions, a sum of steps 1, 2 and 3 minus steps 2′ and 3′. The rate of step 2 corresponds to k_f, whereas the rate of step 2′, to k_r.

The L to M transition is essentially a reversible process, especially at low pH [49,50], and return of the L intermediate back to the initial state was observed in bacteriorhodopsin at low temperatures [51,52], and at room temperature at high values of transmembrane electrochemical gradients where a decrease of quantum efficiency of proton transport was observed in native cells [53] and in oocytes with BR [54] and *Gloeobacter* rhodopsin [55].

Apparently, as in the case of D96N and D96A mutants of BR, the K96A mutation creates a kinetic barrier for proton transfer from the cytoplasmic surface to the Schiff base. However, there is a difference. In BR, these mutations slow but do not eliminate the electric phase correspondent to M decay at neutral pH and even at high pH [46,56]. Upon increasing the pH [56], M decay becomes very slow, comparable or slower than the passive membrane discharge rate so the accurate estimate of the amplitude of ΔΨ becomes difficult at these conditions [56]. For this reason, it was unclear whether D96N and D96A mutations affected overall yield of transmembrane proton transport. However, since positive component corresponding to M decay was observed up to pH 9 [46] and no negative components were reported, one can conclude that

if there was a decrease in efficiency of H^+ pumping, it was not as severe as in K96A of ESR. Careful examination of the photocycle kinetics of the D96N mutant produced evidence for a branch and back reaction from M to BR [57], which suggested some decrease in the efficiency of proton transport in the mutant.

The different pattern of $\Delta\Psi$ in the mutants of the internal proton donor sites, K96A of ESR and D96N or D96A of BR, indicates a larger rate of back reactions in the K96A mutant compared to that in the mutants of BR. This could be caused by two major factors. The first is a larger probability of the shunt reaction from L to the initial state. The second factor is apparently a higher probability of back reaction from M to L, involving reverse proton transfer from Asp85 to the Schiff base. Our hypothesis is that close interaction of Asp85 with His57 in ESR [27] (Fig. 8) provides a potential for a larger possibility of back proton transfer from the Asp85-His57 pair to the Schiff base than in BR, where Asp85 acquires a very high pK_a in M, more than 11 [59,60] from large structural changes involving movement of Arg82 and water molecules [58] and deprotonation of the proton release group [18].

In ESR, mutation of Arg82 does not cause changes in the pK_a of Asp85 similar to that in BR [26]. Its side chain is turned away from Asp85 [27]. This implements His57 as an important factor in tuning the pK_a of Asp85 in the initial state and during the formation of M [26], and in proton release from Asp85 at the end of the photocycle, as also was suggested for proteorhodopsin [22,61]. Moreover, the pH dependence of M accumulation in WT ESR and in the K96A mutant (Fig. 4) indicates that proton transport from the Schiff base to Asp85 is facilitated greatly by deprotonation of some residue, probably His57 or other interacting group X. Comparison of electric potential change at pH 6.5 with kinetics of M rise indicates that there is a positive component preceding formation of M (Fig. 5B), whereas at pH 8.5, a much closer correlation between kinetics of M rise and electrical potential change is observed (Fig. 5D). Thus, besides the electrogenic component associated with the Schiff base-Asp85 proton transfer, at low pH, there is a positive component, which originates from deprotonation of His57 or other interacting group affecting M formation with pK_a ca. 7–7.5, as one can conclude from Fig. 4 and earlier study [30].

It is important to note that in bacteriorhodopsin proton is released during the formation of M. In ESR, proton release at neutral and high pH occurs mostly at the end of the photocycle [26,28] and hence, the output proton pathway in the M state of ESR may retain the proton to the later stages of the photocycle especially at more acidic pH (pH 6.5). In other words, the M state of ESR may contain, partially or completely uncompensated positive charge in the extracellular domain of the protein. It is possible that as a result of this, the energy barrier for the transition of the M intermediate state to the subsequent photocycle intermediates is higher, whereas the energy barrier for the reverse conversion of M to L or K and then back to the initial state correspondingly, is lower, which would lead to a higher probability of the reverse proton transfer reactions and overall lower yield of proton transport.

4.2. Estimations of the fractions of forward and reverse H^+ transfers

The direct and reverse reactions of proton transfer are depicted by arrows in the scheme in Fig. 7. From the ratio of the amplitude of the electrical component, corresponding to M decay in the K96A mutant, $\Delta\Psi_M$, and the total potential $\Delta\Psi_t$ created by a transmembrane H^+ transfer in WT, $\psi_M = \Delta\Psi_M/\Delta\Psi_t$, one can roughly estimate a fraction of molecule, performing forward transmembrane proton transfer, f. We assume that the values of electrogenic components from proton transport between principal sites are proportional to the projections of distances between them on the membrane normal: d_1, between the cytoplasm and the Schiff base; d2, between the Schiff base and Asp85-His57 site, and d_3, between the Asp85-His57 site and the extracellular surface. Since only relative distances matter, one can use relative values ($d_1 + d_2 + d_3 = 1$). From the crystal structure the values of d_1, d_2 and d_3 can be estimated to be ca. 0.54, 0.1 and 0.36, respectively. We will consider three cases for the three pH values.

4.2.1. pH 8.5

At this pH, His57 (or interacting group X) is completely deprotonated in the initial state. Under these conditions the electrical component, corresponding to M decay is a difference between the positive potential created during proton transport in the forward direction through distances d_1 and d_3 minus potential created during reverse transport from Asp85 to the Schiff base and subsequent thermal isomerization to the initial state in the rest of the molecules: $\psi_M = (d_1 + d_3)f - d_2(1 - f)$, or $f = \psi_M + d_2$. At pH 8.5, $\psi_M \sim 0$, and hence $f \sim d_2 = 0.1$. Here we ignored the contribution from small fast negative phases at pH 8.5. If they are taken into account, the fraction of molecules pumping in a forward direction would be even smaller than 10% by a few percentages.

At pH 8.5, only negative electrogenic phase is resolved. It could involve reverse proton transport from Asp85 to the Schiff base. However, it cannot be purely internal proton transport, because it would eliminate the pH dependence of M decay contrary to the data of

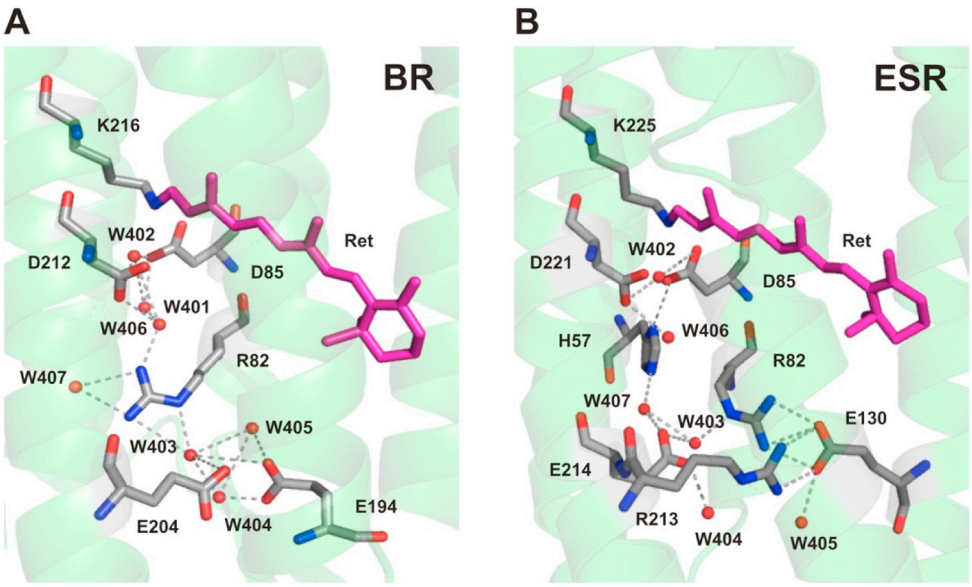

Fig. 8. Comparison of the putative proton pathways in BR and ESR. In BR, the proton is released in M from the proton release group (PRG), a pair of glutamates (Glu194 and Glu204) near the extracellular surface. In ESR, His57 is located close to the primary proton acceptor Asp85 and participates in extensive hydrogen bonded network, which might be involved in release of a proton in the L to M transition at low pH and conductance of a proton from Asp85 to the extracellular side at the end of the photocycle. BR and ESR structures were depicted using PyMol with coordinates obtained from PDB entries 1C3W [58] and 4HYJ [27], respectively.

this and previous studies [28]. Apparently, the reverse reaction is catalyzed by transient protonation of His57 and/or Asp85 from the bulk (steps 2′ and 3′ in Fig. 7). In this case usual pH dependence of M decay should be observed. An example of the effect of transient protonation of the counterion to the Schiff base on the rate and the pH dependence of thermal isomerization of the BR chromophore was described earlier [62].

4.2.2. pH 6.5

At this pH, His (or group X) is almost completely protonated in the initial state and we assume that it deprotonates during formation of M, as suggested earlier [26]. In this case the formula for calculating fraction cycling becomes: $f = \psi_M + d_2 + d_3$. As shown below, it is valid for both possible cases i) when His57 acts as a proton release group and is reprotonated from Asp85 and ii) when it reprotonated from the extracellular side at the end of the photocycle in the reverse transfer.

i) When His (or group X) acts as a proton release group (PRG) it releases a proton during M formation and accepts it from Asp85 at the end of the photocycle. In the fraction of molecules, which are involved in the reverse transport from Asp85 to the Schiff base, it is reprotonated from the extracellular side. A positive potential during the M decay is created by the proton transfer from the cytoplasmic side to the Schiff base in the fraction of the mutant f: ($f * d1$). A negative potential is created by the reprotonation of the Schiff base from Asp85 and reprotonation of His57 from the extracellular side in the $1 - f$ fraction of molecules. It is assumed that both residues (Asp85 and His57) are approximately at the same electric distance from the surface: $\psi_M = fd_1 - (1 - f)d2 - (1 - f)d3$; and then $f = \psi_M + d_2 + d_3$.
ii) The second possibility is that His57 (or close group X) is not a PRG, it simply releases a proton to the extracellular side early in the cycle and reprotonates from the same side during M decay or at the end of the photocycle. A positive potential coupled to the M decay is created during proton transport in the forward direction and is comprised of the sum of d1 and d3 transfer steps in the f fraction of the mutant (performing proton pumping in the right direction), while a negative potential is created in the rest fraction $(1 - f)$ during the reverse transfer from Asp85 to the Schiff base and reprotonation of the His from the extracellular phase in all molecules. Then, $\psi_M = f(d_1 + d_3) - (1 - f)d_2 - d_3$; and $f = \psi_M + d_2 + d_3$ also.

From the measurements, $\psi_M = 0.01$ at pH 6.5 and hence $f = 0.47$. If His57 or group X is closer to the surface (d_3 is less than 0.36), the fraction of forward transfer would be smaller. These estimates are of course approximate but they show how the pH dependence of the fraction pumping can be accounted for and how back reactions affect the amplitude of electrical component accompanying M decay.

4.2.3. pH 7.5

His57 is partially deprotonated (about 50%) at this pH. This situation is described by the combination of the two previous cases with 50% contribution of both: $\psi_M = 0.5[(d_1 + d_3)f - d_2(1 - f)] + 0.5[f(d_1 + d_3) - (1 - f)d_2 - d_3]$; $f = \psi_M + 0.5d_2 + 0.5d_3$. ψ_M for pH 7.5 is in the range of 0.03–0.1. The value for ψ_M is estimated from the relative amplitude of the 138 ms electrogenic phase, so f~0.25–0.32. In other words only ~28% of molecules are involved in direct transport whereas 72% take a reverse, shunt reaction. These estimates correlate with the efficiency of proton transport by K96A mutant in *E. coli* cells being less than 40% of WT at neutral pH but less than 10% at pH above 8 [28]. The data obtained in this study indicate that a decreased rate of proton transport in the mutant and its steeper decline compared to wild type at high pH is caused not only by slowing of the photocycle caused by mutation of the donor but also by a decreased efficiency of direct H^+ transport in K96A from greater contribution of back reactions and associated reverse H^+ transport.

The M intermediate at pH 7.5 exhibits biphasic decay with time constants 25 ms (46%) and 283 ms (54%) apparently from some heterogeneity of the initial population of the protein or the M intermediate possibly from different protonation state of His57. The first component of M decay correlates with a small 25 ms negative phase in potential change (Table S2) which represents some reverse process involving the Schiff base reprotonation from the extracellular side, whereas the second component of M decay is close to 137 ms positive electric phase (Table S2), which at least partially includes direct proton transport from the cytoplasm to the Schiff base. From this the time constant for the reverse non-productive reactions (L, K back to BR) in this fraction can be estimated as ~70–140 ms. When donor is present and reprotonation of the Schiff base occurs within 1 ms, the back reaction with such a time constant and even faster, 25 ms reaction, does not produce significant effect on the overall quantum yield of proton transport, but becomes significant when supply of protons from the cytoplasmic side becomes slower than tens and hundreds of ms. Thus the presence of fast internal donor Lys96 in ESR becomes a factor strongly contributing to efficiency of vectorial transport.

The effect of azide on the recovery of slow electrogenic phases in the K96A mutant is in agreement with this model. Most likely, azide diffuses in the proton channel in a neutral, protonated form, as follows from a titration-like pH dependence of M decay in BR [47]. This results in a reduced electrostatic barrier compared to that for positively charged hydronium ion thus dramatically accelerating delivery of a proton to the Schiff base directly or through water molecules and minimizing probability for back proton transfer from the counterion to the Schiff base.

In conclusion, the measurements of photoinduced electrical potential generation in the photocycle of the K96A mutant of ESR shows that elimination of a proton donor not only slows delivery of protons from the cytoplasmic side to the Schiff base, as in bacteriorhodopsin, but results also in decrease in the yield of overall proton transport. Decrease in the amplitude of positive components of $\Delta\Psi$ generation and appearance of negative electrogenic phases especially at high pH indicates involvement of back reactions, which become significant when the rate of direct reaction involving reprotonation of the Schiff base from the cytoplasmic side of the membrane is dramatically slowed. Addition of azide restores both the rate of direct reactions and the yield of proton transport. A larger impact of back reactions in bacterial pump ESR compared to that in bacteriorhodopsin apparently is from different architecture of the proton acceptor environment and extracellular “half-channel”.

Transparency document

The Transparency document associated with this article can be found, in online version.

Acknowledgements

This work was supported by the grants from RFBR 18-04-00503a, 17-00-00165comfi and Molecular and Cell Biology Program of Russian Academy of Sciences.

Appendix A. Supplementary data

Supplementary data to this article can be found online at https://doi.org/10.1016/j.bbabio.2018.09.365.

References

[1] O. Béjà, E.N. Spudich, J.L. Spudich, M. Leclerc, E.F. Delong, Proteorhodopsin phototrophy in the ocean, Nature 411 (2001) 786–789.
[2] J.C. Venter, K. Remington, J.F. Heidelberg, A.L. Halpern, D. Rusch, J.A. Eisen, D. Wu, I. Paulsen, K.E. Nelson, W. Nelson, D.E. Fouts, S. Levy, A.H. Knap,

M.W. Lomas, K. Nealson, O. White, J. Peterson, J. Hoffman, R. Parsons, H. Baden-Tillson, C. Pfannkoch, Y.-H. Rogers, H.O. Smith, Environmental genome shotgun sequencing of the Sargasso Sea, Science 304 (2004) 66–74.
[3] L.S. Brown, Eubacterial rhodopsins—unique photosensors and diverse ion pumps, Biochim. Biophys. Acta Bioenerg. 1837 (2014) 553–561.
[4] D. Oesterhelt, W. Stoeckenius, Functions of a new photoreceptor membrane, Proc. Natl. Acad. Sci. U. S. A. 70 (1973) 2853–2857.
[5] R.H. Lozier, R.A. Bogomolni, W. Stoeckenius, Bacteriorhodopsin: a light-driven proton pump in *Halobacterium halobium*, Biophys. J. 15 (1975) 955–963.
[6] L.A. Drachev, A.D. Kaulen, L.V. Khitrina, V.P. Skulachev, Fast stages of photoelectric processes in biological membranes. I. Bacteriorhodopsin, Eur. J. Biochem. 117 (1981) 461–470.
[7] R.A. Mathies, S.W. Lin, J.B. Ames, W.T. Pollard, From femtoseconds to biology: mechanism of bacteriorhodopsin's light-driven proton pump, Annu. Rev. Biophys. Biophys. Chem. 20 (1991) 491–518.
[8] T.G. Ebrey, Light energy transduction in bacteriorhodopsin, in: M.B. Jackson (Ed.), Thermodynamics of Membrane Receptors and Channels, CRC Press, Boca Raton, FL, 1993, pp. 353–387.
[9] U. Haupts, J. Tittor, D. Oesterhelt, Closing in on bacteriorhodopsin: progress in understanding the molecule, Annu. Rev. Biophys. Biomol. Struct. 28 (1999) 367–399.
[10] H. Luecke, B. Schobert, H.-T. Richter, J.-P. Cartailler, J.K. Lanyi, Structural changes in bacteriorhodopsin during ion transport at 2 angstrom resolution, Science 286 (1999) 255–260.
[11] J.K. Lanyi, Bacteriorhodopsin, Annu. Rev. Physiol. 66 (2004) 665–688.
[12] O.P. Ernst, D.T. Lodowski, M. Elstner, P. Hegemann, L.S. Brown, H. Kandori, Microbial and animal rhodopsins: structures, functions, and molecular mechanisms, Chem. Rev. 114 (2014) 126–163.
[13] A. Lewis, J. Spoonhower, R.A. Bogomolni, R.H. Lozier, W. Stoeckenius, Tunable laser resonance Raman spectroscopy of bacteriorhodopsin, Proc. Natl. Acad. Sci. U. S. A. 71 (1974) 4462–4466.
[14] M.S. Braiman, T. Mogi, M. Marti, L.J. Stern, H.G. Khorana, K.J. Rothschild, Vibrational spectroscopy of bacteriorhodopsin mutants: light-driven proton transport involves protonation changes of aspartic acid residues 85, 96, and 212, Biochemistry 27 (1988) 8516–8520.
[15] K. Gerwert, G. Souvignier, B. Hess, Simultaneous monitoring of light-induced changes in protein side-group protonation, chromophore isomerization, and backbone motion of bacteriorhodopsin by time-resolved Fourier-transform infrared spectroscopy, Proc. Natl. Acad. Sci. U. S. A. 87 (1990) 9774–9778.
[16] H.G. Khorana, Two light-transducing membrane proteins: bacteriorhodopsin and the mammalian rhodopsin, Proc. Natl. Acad. Sci. U. S. A. 90 (1993) 1166–1171.
[17] A. Dioumaev, H.-T. Richter, L.S. Brown, M. Tanio, S. Tuzi, H. Saito, Y. Kimura, R. Needleman, J.K. Lanyi, Existence of a proton transfer chain in bacteriorhodopsin: participation of Glu-194 in the release of protons to the extracellular surface, Biochemistry 37 (1998) 2496–2506.
[18] S.P. Balashov, Protonation reactions and their coupling in bacteriorhodopsin, Biochim. Biophys. Acta Bioenerg. 1460 (2000) 75–94.
[19] F. Garczarek, L.S. Brown, J.K. Lanyi, K. Gerwert, Proton binding within a membrane protein by a protonated water cluster, Proc. Natl. Acad. Sci. U. S. A. 102 (2005) 3633–3638.
[20] S.P. Balashov, E.S. Imasheva, V.A. Boichenko, J. Antón, J.M. Wang, J.K. Lanyi, Xanthorhodopsin: a proton pump with a light-harvesting carotenoid antenna, Science 309 (2005) 2061–2064.
[21] H. Luecke, B. Schobert, J. Stagno, E.S. Imasheva, J.M. Wang, S.P. Balashov, J.K. Lanyi, Crystallographic structure of xanthorhodopsin, the light-driven proton pump with a dual chromophore, Proc. Natl. Acad. Sci. U. S. A. 105 (2008) 16561–16565.
[22] V.B. Bergo, O.A. Sineshchekov, J.M. Kralj, R. Partha, E.N. Spudich, K.J. Rothschild, J.L. Spudich, His-75 in proteorhodopsin, a novel component in light-driven proton translocation by primary pumps, J. Biol. Chem. 284 (2009) 2836–2843.
[23] L.E. Petrovskaya, E.P. Lukashev, V.V. Chupin, S.V. Sychev, E.N. Lyukmanova, E.A. Kryukova, R.H. Ziganshin, E.V. Spirina, E.M. Rivkina, R.A. Khatypov, L.G. Erokhina, D.A. Gilichinsky, V.A. Shuvalov, M.P. Kirpichnikov, Predicted bacteriorhodopsin from *Exiguobacterium sibiricum* is a functional proton pump, FEBS Lett. 584 (2010) 4193–4196.
[24] D.F. Rodrigues, J. Goris, T. Vishnivetskaya, D. Gilichinsky, M.F. Thomashow, J.M. Tiedje, Characterization of *Exiguobacterium* isolates from the Siberian permafrost. Description of *Exiguobacterium sibiricum* sp. nov, Extremophiles 10 (2006) 285–294.
[25] V.H. Albarracín, I. Kraiselburd, C. Bamann, P.G. Wood, E. Bamberg, M.E. Farias, W. Gärtner, Functional green-tuned proteorhodopsin from modern stromatolites, PLoS One 11 (2016) e0154962.
[26] S.P. Balashov, L.E. Petrovskaya, E.P. Lukashev, E.S. Imasheva, A.K. Dioumaev, J.M. Wang, S.V. Sychev, D.A. Dolgikh, A.B. Rubin, M.P. Kirpichnikov, J.K. Lanyi, Aspartate-histidine interaction in the retinal Schiff base counterion of the light-driven proton pump of *Exiguobacterium sibiricum*, Biochemistry 51 (2012) 5748–5762.
[27] I. Gushchin, P. Chervakov, P. Kuzmichev, A.N. Popov, E. Round, V. Borshchevskiy, A. Ishchenko, L. Petrovskaya, V. Chupin, D.A. Dolgikh, A.S. Arseniev, M. Kirpichnikov, V. Gordeliy, Structural insights into the proton pumping by unusual proteorhodopsin from nonmarine bacteria, Proc. Natl. Acad. Sci. U. S. A. 110 (2013) 12631–12636.
[28] S.P. Balashov, L.E. Petrovskaya, E.S. Imasheva, E.P. Lukashev, A.K. Dioumaev, J.M. Wang, S.V. Sychev, D.A. Dolgikh, A.B. Rubin, M.P. Kirpichnikov, J.K. Lanyi, Breaking the carboxyl rule: lysine 96 facilitates reprotonation of the Schiff base in the photocycle of a retinal protein from *Exiguobacterium sibiricum*, J. Biol. Chem. 288 (2013) 21254–21265.
[29] S.A. Siletsky, M.D. Mamedov, E.P. Lukashev, S.P. Balashov, D.A. Dolgikh, A.B. Rubin, M.P. Kirpichnikov, L.E. Petrovskaya, Electrogenic steps of light-driven proton transport in ESR, a retinal protein from *Exiguobacterium sibiricum*, Biochim. Biophys. Acta Bioenerg. 1857 (2016) 1741–1750.
[30] A.K. Dioumaev, L.E. Petrovskaya, J.M. Wang, S.P. Balashov, D.A. Dolgikh, M.P. Kirpichnikov, J.K. Lanyi, Photocycle of *Exiguobacterium sibiricum* rhodopsin characterized by low-temperature trapping in the IR and time-resolved studies in the visible, J. Phys. Chem. B 117 (2013) 7235–7253.
[31] L.A. Drachev, A.D. Kaulen, A.Y. Semenov, I.I. Severina, V.P. Skulachev, Lipid-impregnated filters as a tool for studying the electric current-generating proteins, Anal. Biochem. 96 (1979) 250–262.
[32] S.A. Siletsky, A.S. Pawate, K. Weiss, R.B. Gennis, A.A. Konstantinov, Transmembrane charge separation during the ferryl-oxo → oxidized transition in a nonpumping mutant of cytochrome c oxidase, J. Biol. Chem. 279 (2004) 52558–52565.
[33] Y.L. Kalaidzidis, A. Gavrilov, P. Zaitsev, A. Kalaidzidis, E. Korolev, PLUK-an environment for software development, Program. Comput. Softw. 23 (1997) 206–211.
[34] D. Zaslavsky, I. Smirnova, S. Siletsky, A. Kaulen, F. Millett, A. Konstantinov, Rapid kinetics of membrane potential generation by cytochrome c oxidase with the photoactive Ru (II)-tris-bipyridyl derivative of cytochrome c as electron donor, FEBS Lett. 359 (1995) 27–30.
[35] S. Siletsky, A.D. Kaulen, A.A. Konstantinov, Resolution of electrogenic steps coupled to conversion of cytochrome c oxidase from the peroxy to the ferryl-oxo state, Biochemistry 38 (1999) 4853–4861.
[36] L. Drachev, A. Kaulen, V. Skulachev, Correlation of photochemical cycle, H+ release and uptake, and electric events in bacteriorhodopsin, FEBS Lett. 178 (1984) 331–335.
[37] A.D. Kaulen, Electrogenic processes and protein conformational changes accompanying the bacteriorhodopsin photocycle, Biochim. Biophys. Acta Bioenerg. 1460 (2000) 204–219.
[38] A.A. Konstantinov, S. Siletsky, D. Mitchell, A. Kaulen, R.B. Gennis, The roles of the two proton input channels in cytochrome c oxidase from *Rhodobacter sphaeroides* probed by the effects of site-directed mutations on time-resolved electrogenic intraprotein proton transfer, Proc. Natl. Acad. Sci. U. S. A. 94 (1997) 9085–9090.
[39] M.D. Mamedov, A.A. Tyunyatkina, S.A. Siletsky, A.Y. Semenov, Voltage changes involving photosystem II quinone–iron complex turnover, Eur. Biophys. J. 35 (2006) 647–654.
[40] S.A. Siletsky, J. Zhu, R.B. Gennis, A.A. Konstantinov, Partial steps of charge translocation in the nonpumping N139L mutant of *Rhodobacter sphaeroides* cytochrome c oxidase with a blocked D-channel, Biochemistry 49 (2010) 3060–3073.
[41] D. Medvedev, E. Medvedev, A. Kotelnikov, A. Stuchebrukhov, Analysis of the kinetics of the membrane potential generated by cytochrome c oxidase upon single electron injection, Biochim. Biophys. Acta Bioenerg. 1710 (2005) 47–56.
[42] S.A. Siletsky, D. Han, S. Brand, J.E. Morgan, M. Fabian, L. Geren, F. Millett, B. Durham, A.A. Konstantinov, R.B. Gennis, Single-electron photoreduction of the P M intermediate of cytochrome c oxidase, Biochim. Biophys. Acta Bioenerg. 1757 (2006) 1122–1132.
[43] S.A. Siletsky, Steps of the coupled charge translocation in the catalytic cycle of cytochrome c oxidase, Front. Biosci. (Landmark Ed.) 18 (2013) 36–57.
[44] A. Miller, D. Oesterhelt, Kinetic optimization of bacteriorhodopsin by aspartic acid 96 as an internal proton donor, Biochim. Biophys. Acta Bioenerg. 1020 (1990) 57–64.
[45] J. Tittor, C. Soell, D. Oesterhelt, H. Butt, E. Bamberg, A defective proton pump, point-mutated bacteriorhodopsin Asp96 → Asn is fully reactivated by azide, EMBO J. 8 (1989) 3477–3482.
[46] H. Otto, T. Marti, M. Holtz, T. Mogi, M. Lindau, H.G. Khorana, M.P. Heyn, Aspartic acid-96 is the internal proton donor in the reprotonaion of the Schiff base of bacteriorhodopsin, Proc. Natl. Acad. Sci. U. S. A. 86 (1989) 9228–9232.
[47] L.S. Brown, J.K. Lanyi, Determination of the transiently lowered pK_a of the retinal Schiff base during the photocycle of bacteriorhodopsin, Proc. Natl. Acad. Sci. U. S. A. 93 (1996) 1731–1734.
[48] S.V. Danshina, L.A. Drachev, A.D. Kaulen, H.G. Khorana, T. Marti, T. Mogi, V.P. Skulachev, The mechanism of the H^+ transport by bacteriorhodopsin: a study on Asp-96 mutants, Biochem. Mosc. 57 (1992) 1574–1585.
[49] R. Lozier, A. Xie, J. Hofrichter, G.M. Clore, Reversible steps in the bacteriorhodopsin photocycle, Proc. Natl. Acad. Sci. U. S. A. 89 (1992) 3610–3614.
[50] L. Zimanyi, G. Varo, M. Chang, B. Ni, R. Needleman, J.K. Lanyi, Pathways of proton release in the bacteriorhodopsin photocycle, Biochemistry 31 (1992) 8535–8543.
[51] F.F. Litvin, S.P. Balashov, V.A. Sineshchekov, The investigation of the primary photochemical conversions of bacteriorhodopsin in purple membranes and cells of *Halobacterium halobium* by the low temperature spectrophotometry method, Bioorg. Khim. 1 (1975) 1767–1777.
[52] T. Iwasa, F. Tokunaga, T. Yoshizawa, A new pathway in the photoreaction cycle of trans-bacteriorhodopsin and the absorption spectra of its intermediates, Biophys. Struct. Mech. 6 (1980) 253–270.
[53] V.T. Dubrovskii, S.P. Balashov, O.A. Sineshchekov, L.N. Chekulaeva, F.F. Litvin, Photoinduced changes in the quantum yields of the photochemical cycle of conversions of bacteriorhodopsin and transmembrane transport of protons in *Halobacterium halobium* cells, Biochem. Mosc. 47 (1982) 1036–1046.
[54] G. Nagel, B. Kelety, B. Möckel, G. Büldt, E. Bamberg, Voltage dependence of proton pumping by bacteriorhodopsin is regulated by the voltage-sensitive ratio of M1 to M2, Biophys. J. 74 (1998) 403–412.
[55] A. Vogt, J. Wietek, P. Hegemann, Gloeobacter rhodopsin, limitation of proton pumping at high electrochemical load, Biophys. J. 105 (2013) 2055–2063.
[56] M. Holz, L.A. Drachev, T. Mogi, H. Otto, A.D. Kaulen, M.P. Heyn, V.P. Skulachev,

H.G. Khorana, Replacement of aspartic acid-96 by asparagine in bacteriorhodopsin slows both the decay of the M intermediate and the associated proton movement, Proc. Natl. Acad. Sci. U. S. A. 86 (1989) 2167–2171.
[57] L. Zimányi, Á. Kulcsár, J.K. Lanyi, D.F. Sears, J. Saltiel, Intermediate spectra and photocycle kinetics of the Asp96 → Asn mutant bacteriorhodopsin determined by singular value decomposition with self-modeling, Proc. Natl. Acad. Sci. U. S. A. 96 (1999) 4414–4419.
[58] H. Luecke, B. Schobert, H.-T. Richter, J.-P. Cartailler, J.K. Lanyi, Structure of bacteriorhodopsin at 1.55 Å resolution, J. Mol. Biol. 291 (1999) 899–911.
[59] M.S. Braiman, A.K. Dioumaev, J.R. Lewis, A large photolysis-induced pKa increase of the chromophore counterion in bacteriorhodopsin: implications for ion transport mechanisms of retinal proteins, Biophys. J. 70 (1996) 939–947.
[60] A. Dioumaev, Infrared methods for monitoring the protonation state of carboxylic amino acids in the photocycle of bacteriorhodopsin, Biochem. Mosc. 66 (2001) 1269–1276.
[61] F. Hempelmann, S. Holper, M.K. Verhoefen, A.C. Woerner, T. Kohler, S.A. Fiedler, N. Pfleger, J. Wachtveitl, C. Glaubitz, His75-Asp97 cluster in green proteorhodopsin, J. Am. Chem. Soc. 133 (2011) 4645–4654.
[62] S.P. Balashov, E.S. Imasheva, R. Govindjee, T.G. Ebrey, Titration of aspartate-85 in bacteriorhodopsin: what it says about chromophore isomerization and proton release, Biophys. J. 70 (1996) 473–481.